Available online at www.sciencedirect.com

SCIENCE DIRECT®

Journal of Nuclear Materials 355 (2006) 163–170

journal of nuclear materials

www.elsevier.com/locate/jnucmat

Dysprosium hafnate as absorbing material for control rods

V.D. Risovany *, A.V. Zakharov, E.M. Muraleva, V.M. Kosenkov, R.N. Latypov

Dimitrovgrad-10, Ulyanovsk region, Federal State Unitary Enterprise, 'State Scientific Center Research Institute of Atomic Reactors' (FSUE SSC RIAR), Russian Federation

Received 17 October 2005; accepted 9 May 2006

Abstract

Dysprosium hafnate is proposed as a promising absorbing material for control rods of thermal nuclear reactors. The properties of dysprosium hafnate pellets with different Dy and Hf contents are presented in this article. The fluorite phase is characterized by the density range 6.8–7.8 g/cm^3 and; the thermal diffusivity achieves 0.58–0.83 mm^2/s at 20 °C, thermal conductivity of 1.5–2.0 W/(K m) and TLEC of $(8.4–8.6) \times 10^{-6}$ K^{-1} at 20 °C. The temperature dependence of the thermophysical properties of dysprosium hafnate are presented. The neutron absorption efficiency of dysprosium hafnate was estimated in comparison with boron carbide. The radiation resistance of pellets after irradiation in the BOR-60 reactor is presented as well.

1. Introduction

Dysprosium titanate powder of 4.9–5.3 g/cm^3 density is used in the Russian thermal reactors. Dysprosium titanate possesses higher radiation resistance as compared with boron carbide and does not form any gaseous products when burning up [1]. However, the dysprosium titanate structure is sensitive to composition changes caused by synthesis that complicates its production technology. A phase formed as a result of deviations from the initial composition of the synthesized compound has lower radiation resistance as compared with the fluorite-like phase [2]. Therefore, there is an urgent task to find compact absorbing materials as an alternative to dysprosium titanate and boron carbide that possess higher density, good thermophysical properties, sufficient physical efficiency and radiation resistance.

The most promising absorbing materials are solid fluorite-type solutions in the Dy_2O_3–HfO_2 system. Compounds formed in this system contain isotopes of two absorbing elements: Dy and Hf that increases additionally the physical efficiency of the material. The application of dysprosium hafnate pellets allows the absorber density to be increased up to 7–8 g/cm^3 (70–75% of theoretical density).

This paper presents the examination results of a new promising dysprosium hafnate absorbing material, its initial operating characteristics and some experimental results as well.

---

* Corresponding author. Tel.: +7 84235 65562.
E-mail address: fae@niiar.ru (V.D. Risovany).

0022-3115/$ - see front matter © 2006 Elsevier B.V. All rights reserved.
doi:10.1016/j.jnucmat.2006.05.029

2. Materials under testing

Dysprosium hafnate pellets were fabricated to study the material properties and for irradiation tests. These pellets were made from a mixture of Dy_2O_3, HfO_2 and Nb_2O_5 powders by solid-phase synthesis. Nb_2O_5 was used as stabilizing addition. The characteristics of the studied pellets are presented in Table 1.

To perform irradiation tests the pellets were placed in specially made capsules (dummies), which represent a steel 08Cr18Ni10Ti cladding, 8.2 mm in diameter and 4.5 mm thick. The capsules were sealed by end plugs (Fig. 1). The capsules 88 mm long were filled with dysprosium hafnate pellets.

Table 1
Characteristics of dysprosium hafnate pellets

No.	Composition, mol%	Geometry, mm		Density, g/cm^3
		Diameter	Height	
1	Dy_2O_3 – 75, HfO_2 – 23, Nb_2O_5 – 2	6.98	7.8	6.8–7.1
2	Dy_2O_3 – 49, HfO_2 – 49, Nb_2O_5 – 2	6.65	7.4	7.0–7.2
3	Dy_2O_3 – 23, HfO_2 – 75, Nb_2O_5 – 2	6.65	7.5	7.4–7.8

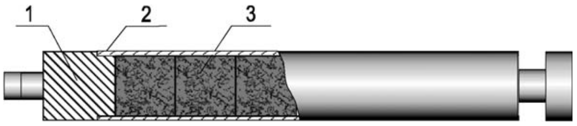

Fig. 1. Design of a dummy with dysprosium titanate pellets: 1 – end plugs; 2 – cladding; 3 – absorbing core.

3. Dysprosium hafnate structure

Fig. 2 presents the phase diagram of the Dy_2O_3–HfO_2 system. Solid fluorite-type solutions are formed at temperatures below 1000 °C and 12–55 mol.% Dy_2O_3, solid C-type cubic solutions (and derivatives from the fluorite structure as well) are formed at and above 75 mol.% Dy_2O_3, and their two-phase mixture in the range 55–75 mol.% Dy_2O_3. All these solution types and their mixtures possess high radiation resistance due to a large number of stoichiometric vacancies in their structure.

4. Initial operating characteristics

The dysprosium hafnate microstructures of different composition do not differ significantly and are characterized by a uniform porosity with pore diameters 10–30 μm (Fig. 3). The X-ray diffraction analysis of dysprosium hafnate showed the presence of reflexes of the fluorite-type structure (Fig. 4) having the crystalline lattice parameters presented in Table 2.

A ‘flash’ method was used to determine the thermal diffusivity of the dysprosium hafnate samples tested up to 600 °C [5]. Fig. 5 presents the results of the thermal diffusivity measurement. Sample no. 1 possesses the highest thermal diffusivity. The difference between thermal diffusivity of samples no. 2 and no. 3 is insignificant and makes up 7–10% within the whole examined temperature range.

The thermal diffusivity of dysprosium hafnate samples decreases with the temperature rise up to 400 °C that is related to the effect of the electron conductivity mechanisms. These mechanisms are

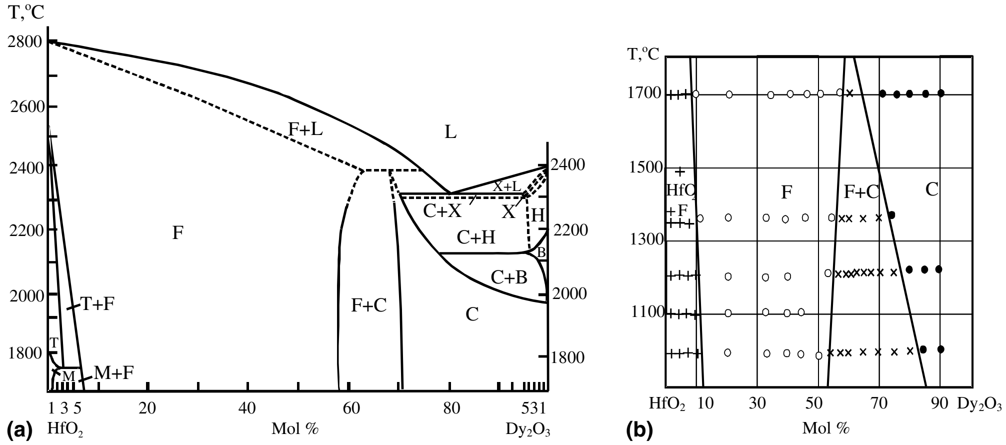

Fig. 2. Phase diagram of the Dy_2O_3–HfO_2 system (a) [3], (b) [4]: F – fluorite, C – cubic structure of Dy_2O_3.

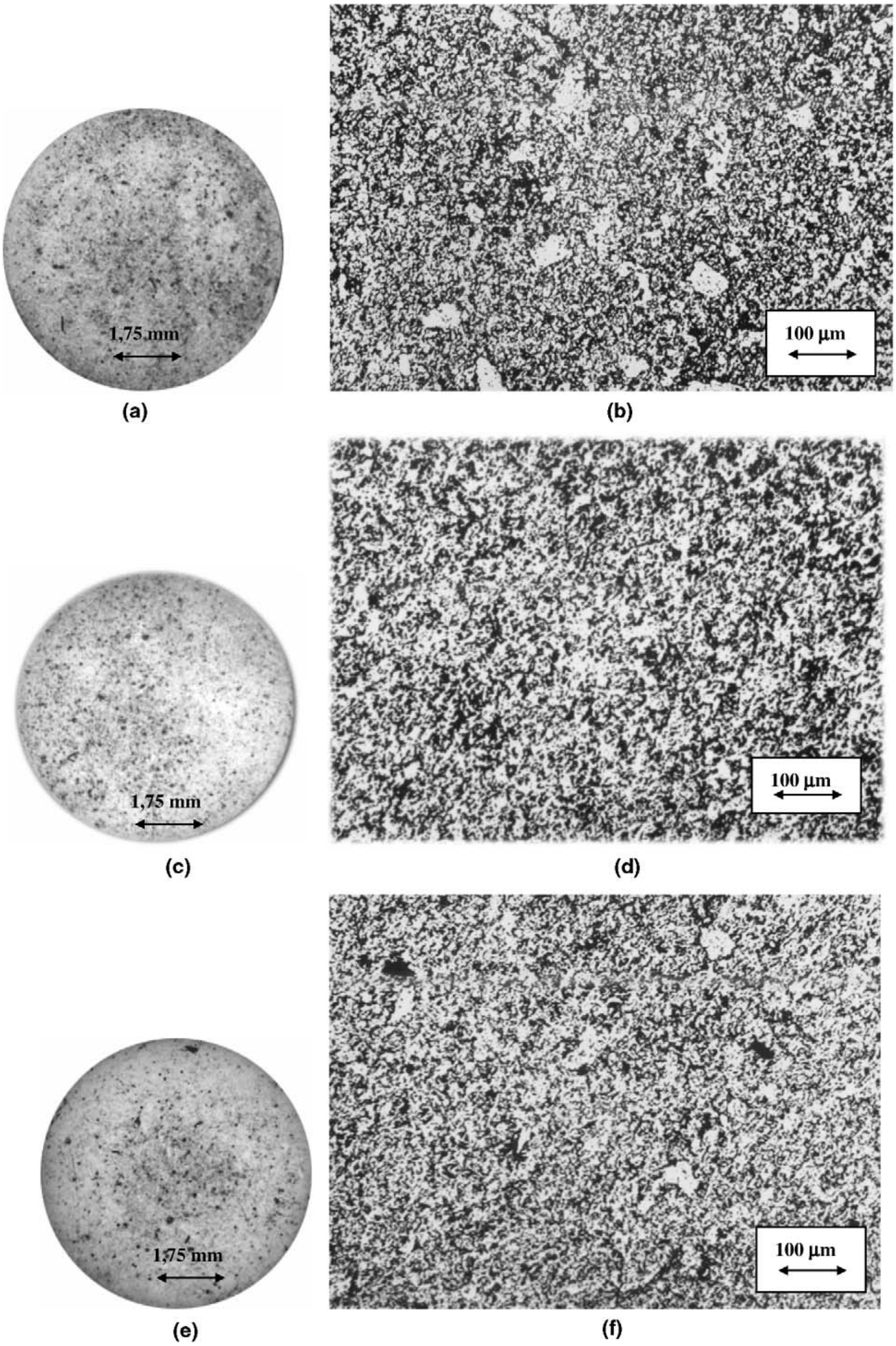

Fig. 3. Macro- (a), (c), (e) and micro-structure (b), (d), (f) of dysprosium hafnate pellets: (a) and (b) Dy_2O_3 – 75 mol.%, HfO_2 – 23 mol.%, Nb_2O_5 – 2 mol.%; (c) and (d) Dy_2O_3 – 49 mol.%, HfO_2 – 49 mol.%, Nb_2O_5 – 2 mol.%; (e) and (f) Dy_2O_3 – 23 mol.%, HfO_2 – 75 mol.%, Nb_2O_5 – 2 mol.%.

characterized by the increase of the thermal resistance with the temperature rise and, consequently, by the decrease of the thermal diffusivity [6]. At temperatures higher than 400 °C the thermal diffusivity increases that is characterized by a dominant influence of the photon conductivity mechanisms [5].

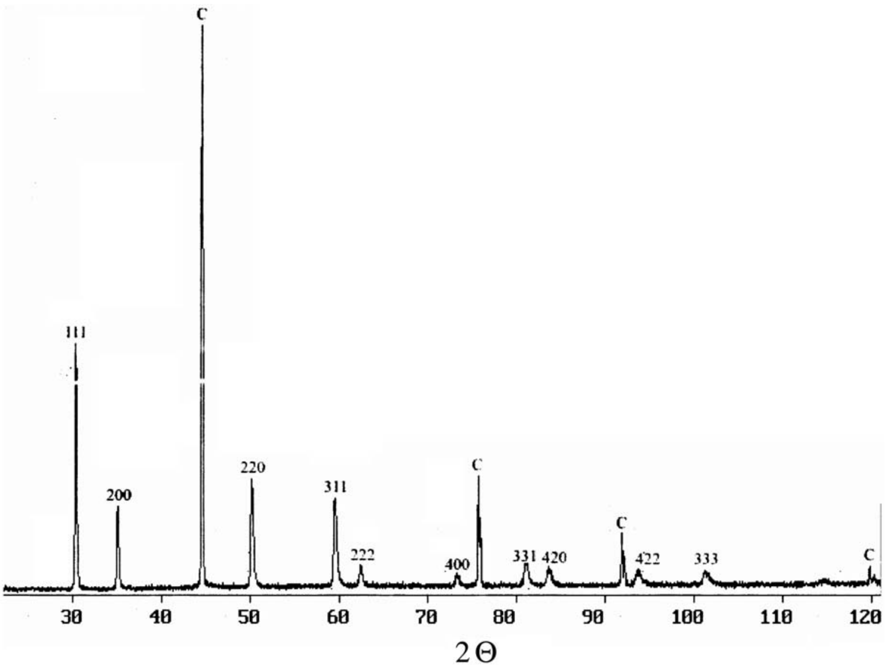

Fig. 4. Typical diffractogram of dysprosium hafnate pellets (C-standard line of diamond).

Table 2
Crystalline lattice parameters of dysprosium hafnate pellets

No.	Composition, mol.%	Lattice spacing, nm
1	Dy_2O_3 – 75, HfO_2 – 23, Nb_2O_5 – 2	$a = (0.51875 \pm 0.00012)$
2	Dy_2O_3 – 49, HfO_2 – 49, Nb_2O_5 – 2	$a = (0.52311 \pm 0.00012)$
3	Dy_2O_3 – 23, HfO_2 – 75, Nb_2O_5 – 2	$a = (0.51869 \pm 0.00012)$

The heat capacity of the dysprosium hafnate samples was measured by the dynamic C-calorimeter method at the IT-C-400 facility (Fig. 6). The principle of the heat capacity measurement is that the thermal flux passing through the middle cross-section of the calorimeter heats the sample and capsule under testing. The thermal flux value passing through the calorimeter is estimated by the temper-

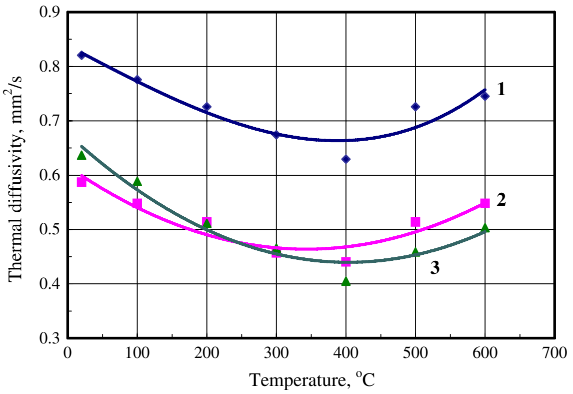

Fig. 5. Thermal diffusivity of dysprosium hafnate pellets: 1 – Dy_2O_3 – 75 mol.%, HfO_2 – 23 mol.%, Nb_2O_5 – 2 mol.% (25 ± 3% of porosity); 2 – Dy_2O_3 – 49 mol.%, HfO_2 – 49 mol.%, Nb_2O_5 – 2 mol.% (24 ± 4% of porosity); 3 – Dy_2O_3 – 23 mol.%, HfO_2 – 75 mol.%, Nb_2O_5 – 2 mol.% (25 ± 3% of porosity).

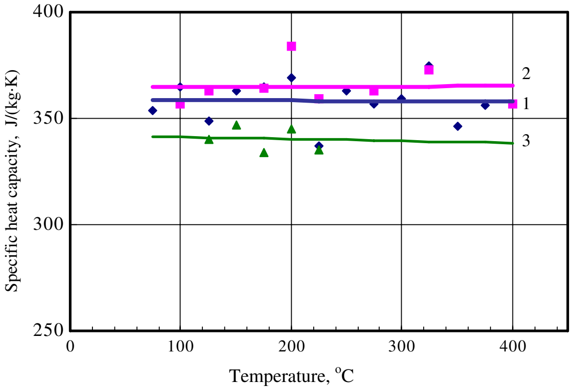

Fig. 6. Heat capacity of dysprosium hafnate pellets: 1 – Dy_2O_3 – 75 mol.%, HfO_2 – 23 mol.%, Nb_2O_5 – 2 mol.% (25 ± 3% of porosity); 2 – Dy_2O_3 – 49 mol.%, HfO_2 – 49 mol.%, Nb_2O_5 – 2 mol.% (24 ± 4% of porosity); 3 – Dy_2O_3 – 23 mol.%, HfO_2 – 75 mol.%, Nb_2O_5 – 2 mol.% (25 ± 3% of porosity).

ature drop on the calorimeter and its thermal conductivity determined on the basis of independent calibration experiments with a copper sample. The temperature range is up to 400 °C. The method error is less than 6%. The pellet heat capacity is practically constant within the whole temperature range under examination.

Thermal conductivity was estimated on the basis of known values of thermal diffusivity, heat capacity and density (Fig. 7). The temperature dependence of the change of thermal diffusivity and thermal conductivity of dysprosium hafnate is identical, is can be explained by the constant values of heat capacity within the examined temperature range as well as by an insignificant difference of the heat capacity values from the chemical composition.

The linear thermal expansion coefficient (LTEC) was measured with a special facility by varying the constant rate of the sample temperature change from 1 to 10 °C/min. The sample elongation was constantly recorded by an inductive sensor with an accuracy of 0.001 mm. The LTEC measurement error made up $0.2 \times 10^{-6}\,K^{-1}$ at temperatures higher than 100 °C. Table 3 presents the LTEC measurement results at 20 °C and 500 °C.

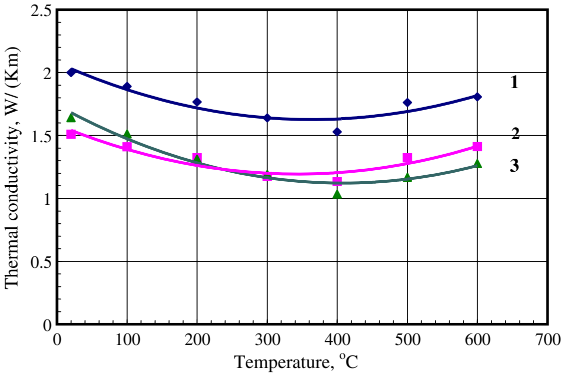

Fig. 7. Thermal conductivity dysprosium hafnate pellets: 1 – Dy_2O_3 – 75 mol.%, HfO_2 – 23 mol.%, Nb_2O_5 – 2 mol.% (25 ± 3% of porosity); 2 – Dy_2O_3 – 49 mol.%, HfO_2 – 49 mol.%, Nb_2O_5 – 2 mol.% (24 ± 4% of porosity); 3 – Dy_2O_3 – 23 mol.%, HfO_2 – 75 mol.%, Nb_2O_5 – 2 mol.% (25 ± 3% of porosity).

Table 3
Linear thermal expansion coefficient (LTEC) of dysprosium hafnate pellets

No.	Composition, mol%	TLEC × 10^{-6}, K^{-1}	
		20 °C	500 °C
1	Dy_2O_3 – 75, HfO_2 – 23, Nb_2O_5 – 2	8.5	11.6
2	Dy_2O_3 – 49, HfO_2 – 49, Nb_2O_5 – 2	8.6	11.1
3	Dy_2O_3 – 23, HfO_2 – 75, Nb_2O_5 – 2	8.4	11.5

5. Absorption efficiency

There are two neutron absorbers, Dy and Hf, in the Dy_2O_3–HfO_2 system that have high macroscopic cross-sections of thermal neutron absorption (Fig. 8). Ta and W are hafnium decay products; Ho and Er are those of dysprosium decay. These elements are also able to absorb neutrons. The absorption cross-sections of dysprosium isotopes are from 130 barn to 2600 barn (Fig. 8(a)). The region of resonance absorption is 1.5–50 eV, in which absorption cross-section can achieve about 1000 barn (Fig. 8(a)).

The region of neutron resonance absorption of hafnium is twice wider, from 1 eV to 200 eV, that is approximately equal to neutron absorption cross-sections of dysprosium (up to 10000 barn in some cases) (Fig. 8(b)) but its thermal absorption cross-section is significantly smaller than that of dysprosium and makes up 14–1500 barn (Fig. 8(b)), the average value being equal to 107 barn only.

At the same time, the integral values of the neutron absorption efficiency in the energy region typical for thermal reactors are comparable for hafnium and dysprosium [8]. These values are 15–20% lower than those for boron carbide of 1.8 g/cm^3 density with a natural content of ^{10}B and ^{11}B isotopes and europium having a density higher than 3 g/cm^3.

Dysprosium hafnate has a significantly wider region of resonance absorption in combination with high dysprosium cross-sections of thermal neutron absorption. This conclusion is confirmed experimentally (Fig. 9). The addition of ≈20% of dysprosium to hafnium allowed the increase of its relative efficiency from 0.595 to 0.636 (by ≈8%) for cores with intermediate neutron spectrum and from 0.808 to 0.846 (by ≈5%) for the VVER (PWR) cores (B_4C reference of 1.81 g/cm^3 density with a natural content of ^{10}B and ^{11}B isotopes was used; efficiency was taken as 1.000).

6. Irradiation tests

The irradiation tests of capsules with pellets from dysprosium hafnate were performed in the

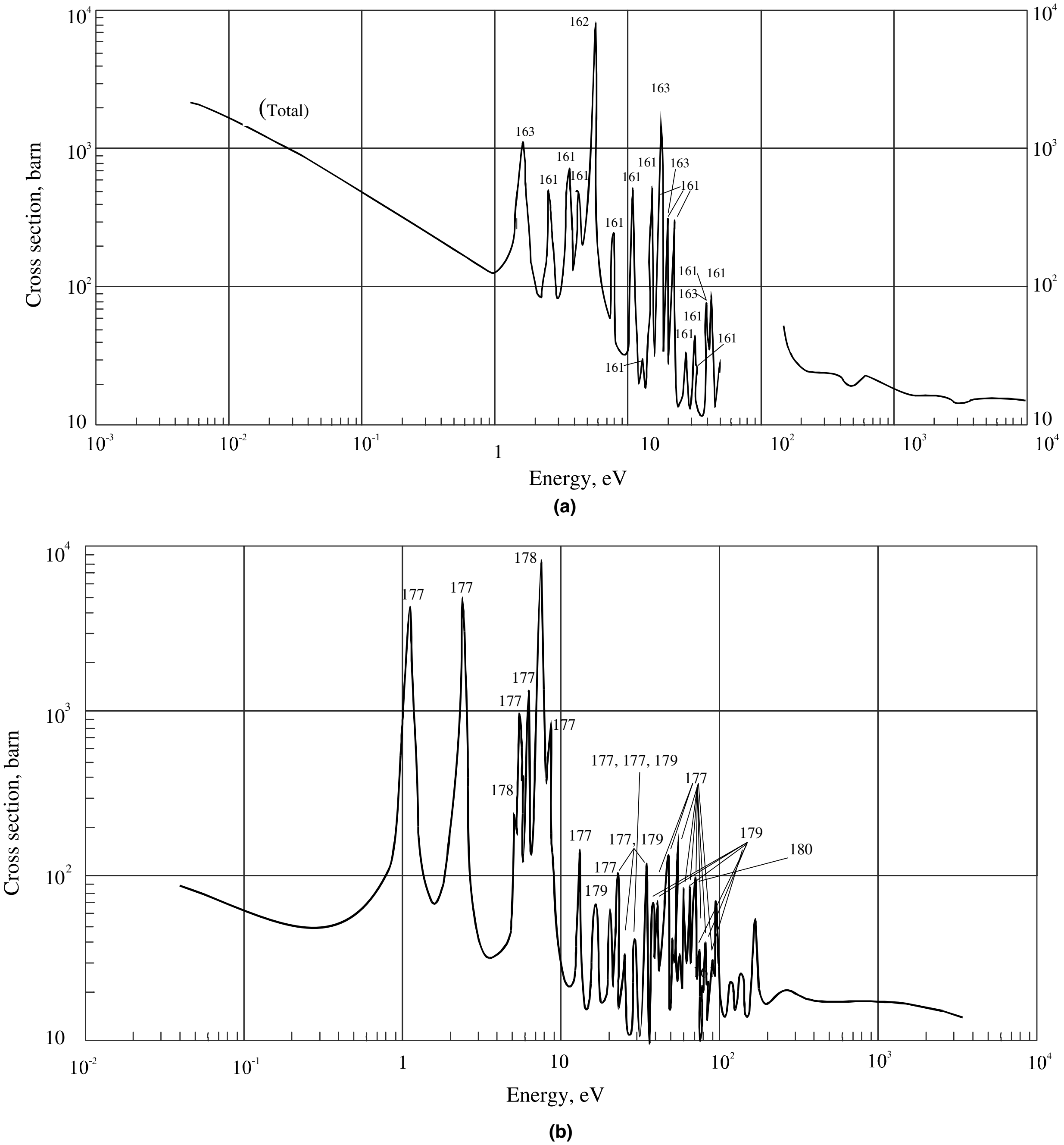

Fig. 8. Neutron cross-section of Dy (a) and Hf (b) versus neutron energy [7].

irradiation rig located in the material science assembly of the BOR-60 reactor. The irradiation rig represented a pipe from Cr18Ni10Ti steel, 39.5 mm in diameter, 0.8 mm thick and 455 mm long. Inside this pipe and parallel to its axis tubes from EU-847 stainless steel and 12 × 0.5 mm in diameter were located. Capsules with absorbing materials were placed inside these tubes.

The maximal fast neutron fluence achieved 1.0×10^{22} cm^{-2}. The sodium temperature at the assembly inlet made up 330–340 °C and that one at the assembly outlet 360–370 °C. The calculated

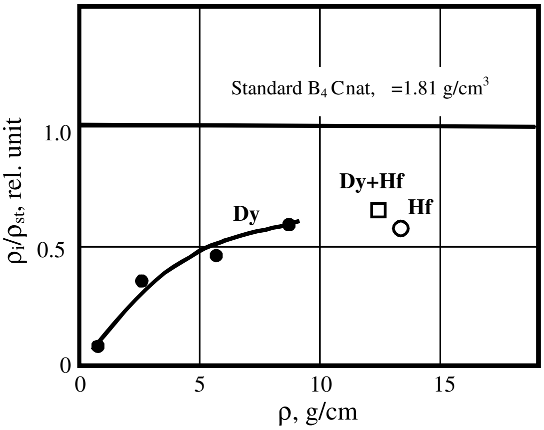

Fig. 9. Dependence of the Dy, Hf, Dy + Hf efficiency on the density at intermediate neutron spectrum (nuclear density of Hf – 4.38 barn; in the Hf + Dy composition 3.06 barn and 0.66 barn, respectively).

temperature of the dysprosium hafnate samples made up 350–450 °C.

The capsules preserved their integrity after irradiation. No swelling and cladding deformation as well as the diameter increase was observed [9]. All the dysprosium hafnate pellets could be freely removed from capsules after irradiation when cutting off the end plugs. They also preserved their shape and integrity. Their appearance did not differ from that of the unirradiated samples. No changes of the pellet geometric dimensions were observed.

The macro- and micro-structures of pellets after irradiation are presented in Fig. 10.

The X-ray diffraction analysis revealed the distorted material structure that resulted in the widening and decrease of diffraction lines. The crystalline structure did not change; the lattice spacing increased by 0.2%; the lattice volume increased by 0.6% [9].

7. Conclusion

The dysprosium hafnate pellets are proposed as a new promising absorbing material for thermal reactors. The technology for solid-phase synthesis of dysprosium hafnate of different composition with a fluorite structure is mastered.

The operating characteristics of unirradiated dysprosium hafnate pellets were examined. The presence of a fluorite-type structure, higher density and thermal characteristics make this new absorbing material more attractive as compared with dysprosium titanate.

The PIE of the dysprosium hafnate pellets irradiated in the BOR-60 reactor up to a neutron fluence of 1×10^{22} cm^{-2} showed the following:

- capsules preserved their integrity and geometric dimensions;
- dysprosium hafnate pellets preserved their integrity and geometric dimensions;
- dysprosium hafnate pellets preserved their crystalline structure;
- increase of the crystalline lattice parameter did not exceed 0.06%.

The examinations of the dysprosium hafnate pellets before and after irradiation confirmed their high radiation resistance within the required range of neutron fluence and temperature.

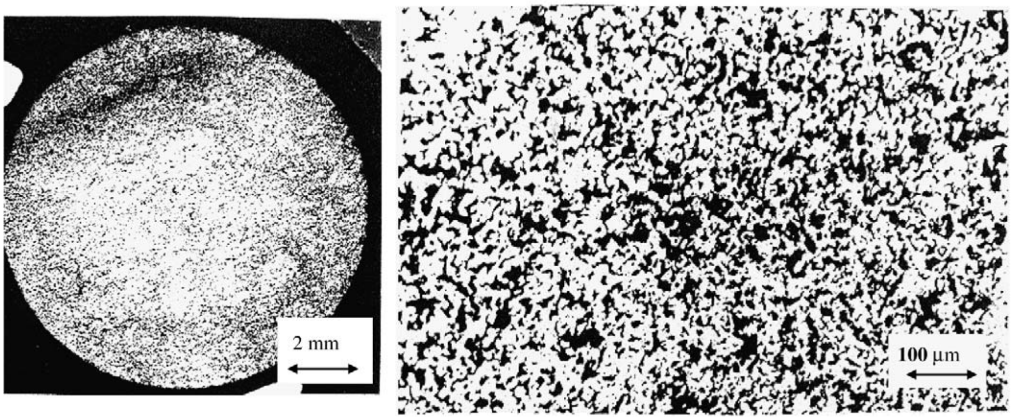

Fig. 10. Macro- and micro-structure of dysprosium hafnate pellets after irradiation.

Acknowledgements

The authors wish to express their appreciation to V. Sandakov (FSUE SSC RIAR) for his assistance in preparing this paper.

References

[1] V.D. Risovany, E.E. Varlashova, D.N. Suslov, J. Nucl. Mater. 281 (2000) 84.
[2] V.M. Koshkin, U.N. Dmitriev, U.R. Zabrodski, R.L. Tarnopolskaia, Y.A. Ylmanic, Physics and Technique of Semiconductors, vol. 18, part 8, 1984, p. 1373.
[3] A.V. Shevchenko, A.V. Lopato, L.V. Nazarenko, Inorg. Mater. 20 (1984) 1862.
[4] E.B. Perova, L.N. Spiridonov, L.N. Komisarova, Inorg. Mater. 8 (1972) 1878.
[5] W.J. Parker, R.J. Jenkins, C.P. Butler, G.L. Abbott, J. Appl. Phys. 32 (1961) 1679.
[6] A. Misnar, Thermal Conductivity of Solids, Liquids, Gases and Their Compositions, Mir, Moscow, 1968.
[7] R.A. Murgatroyd, B.T. Kelly, At. Energy Rev. 15 (1) (1977) 3.
[8] V.D. Risovany, A.V. Zakharov, E.P. Klochkov, T.M. Guseva, Boron in nuclear engineering, Dimitrovgrad: FSUE 'SSC RIAR', 2003, p. 345.
[9] V.D. Risovany, A.V. Zaharov, E.P. Klochkov, E.E. Varlashova, D.N. Suslov, A.B. Ponomarenko, A.V. Scheglov, Dysprosium and hafnium-based absorbers for advanced WWER control rods, Technical committee meeting and assembly materials for water reactors: experience, performance and perspectives, IAEA 1998, IAEA-TECDOC-1132, 2000, p. 91.